Report

Current Biology

Prolific Origination of Eyes in Cnidaria with Co-option of Non-visual Opsins

Graphical Abstract

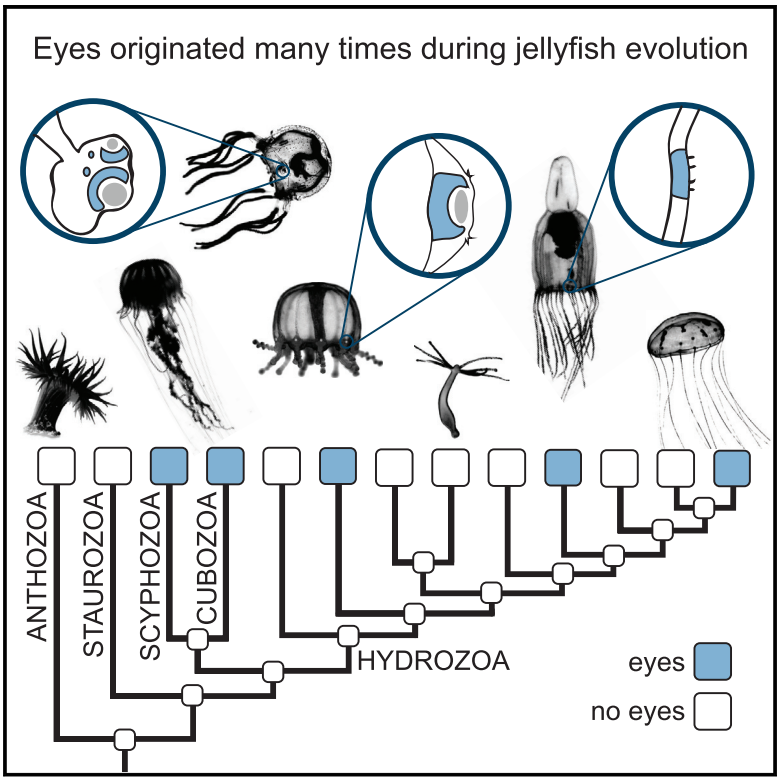

Highlights

- Jellyfish eyes (eyespots, pigment cups, and lensed-eyes) originated multiple times
- Known morphological differences are consistent with multiple eye origins
- Expression of photosensitive proteins supports separate eye origins

Authors

Natasha Picciani, Jamie R. Kerlin, Noemie Sierra, ..., Johanna T. Cannon, Marymegan Daly, Todd H. Oakley

Correspondence

natasha.picciani@lifesci.ucsb.edu (N.P.), oakley@lifesci.ucsb.edu (T.H.O.)

In Brief

Picciani et al. find that eyes evolved separately many times during jellyfish evolution. Their results are based on broad phylogenetic trees of Cnidarians and their photosensitive opsin proteins and show that known morphological differences in eyes and expression of opsins are consistent with multiple eye origins.

Picciani et al., 2018, Current Biology *28*, 2413–2419
August 6, 2018 © 2018 Elsevier Ltd.
https://doi.org/10.1016/j.cub.2018.05.055

CellPress

Current Biology
Report

CellPress

Prolific Origination of Eyes in Cnidaria with Co-option of Non-visual Opsins

Natasha Picciani,[1,*] Jamie R. Kerlin,[1] Noemie Sierra,[1] Andrew J.M. Swafford,[1] M. Desmond Ramirez,[1,3] Nickellaus G. Roberts,[1] Johanna T. Cannon,[1] Marymegan Daly,[2] and Todd H. Oakley[1,4,*]
[1]Department of Ecology, Evolution and Marine Biology, University of California, Santa Barbara, Santa Barbara, CA 93106, USA
[2]Department of Evolution, Ecology, and Organismal Biology, Ohio State University, Columbus, OH 43210, USA
[3]Present address: Department of Biology, University of Massachusetts, Amherst, Amherst, MA 01003, USA
[4]Lead Contact
*Correspondence: natasha.picciani@lifesci.ucsb.edu (N.P.), oakley@lifesci.ucsb.edu (T.H.O.)
https://doi.org/10.1016/j.cub.2018.05.055

SUMMARY

Animal eyes vary considerably in morphology and complexity and are thus ideal for understanding the evolution of complex biological traits [1]. While eyes evolved many times in bilaterian animals with elaborate nervous systems, image-forming and simpler eyes also exist in cnidarians, which are ancient non-bilaterians with neural nets and regions with condensed neurons to process information. How often eyes of varying complexity, including image-forming eyes, arose in animals with such simple neural circuitry remains obscure. Here, we produced large-scale phylogenies of Cnidaria and their photosensitive proteins and coupled them with an extensive literature search on eyes and light-sensing behavior to show that cnidarian eyes originated at least eight times, with complex, lensed-eyes having a history separate from other eye types. Compiled data show widespread light-sensing behavior in eyeless cnidarians, and comparative analyses support ancestors without eyes that already sensed light with dispersed photoreceptor cells. The history of expression of photoreceptive opsin proteins supports the inference of distinct eye origins via separate co-option of different non-visual opsin paralogs into eyes. Overall, our results show eyes evolved repeatedly from ancestral photoreceptor cells in non-bilaterian animals with simple nervous systems, co-opting existing precursors, similar to what occurred in Bilateria. Our study underscores the potential for multiple, evolutionarily distinct visual systems even in animals with simple nervous systems.

RESULTS AND DISCUSSION

Traits like eyes have long challenged biologists to explain steps leading to the evolution of complexity [1]. Animal eyes are made of smaller building blocks, minimally including photoreceptor cells and pigment cells and sometimes having lenses or mirrors for improved spatial resolution. Components of eyes are recognizable across vast evolutionary distances, leading to hypotheses that the parts accrued gradually to evolve complex eyes. Eye evolution is primarily informed by studies of bilaterian animals (arthropods, molluscs, and vertebrates), which almost invariably evolved with sophisticated neural machinery to process visual information. Yet eyes also exist in Cnidaria (jellyfishes, corals, and sea anemones), which are ancient non-bilaterians with nervous systems of dispersed and condensed neurons for locally processing information and no typical bilaterian central nervous system (but see [2]).

The number of times eyes originated in this ancient animal group with simple nervous systems remains unresolved. Cnidarian eyes express transcription factors homologous to those expressed in bilaterian eyes, leading to claims of a single origin of all eyes, including those of cnidarians [3]. However, cnidarians also show differences in structural details of photoreceptors, leading to suggestions of four or five origins of eyes within Cnidaria [4]. Finally, a morphological phylogeny of major cnidarian groups using eyes as one of many traits suggests eyes appeared at least twice in Cnidaria [5]. Overall, cnidarian eye evolution remains controversial because previous studies were either non-phylogenetic or lacked the extensive taxon sampling necessary to address origins of eyes in a group as diverse and variable as Cnidaria.

Phylogenetic Support for Multiple Origins of Eyes among Adult Pelagic Medusa

To address questions of eye evolution in an ancient group with simpler nervous systems, we produced a large-scale molecular phylogeny of Cnidaria (1,102 species) and performed ancestral state estimation with parsimony, maximum likelihood (ML), and Bayesian approaches, using extensive data on presence of eyes gathered from published literature for adult medusae (Table S1). An eye is minimally defined as a region made of photoreceptor cells adjacent to pigment cells [6]. Some researchers restrict the term eyes to image-forming organs and use ocelli for those that do not form images [7]. But morphological variation among ocelli and eyes typically forms a continuous gradation, making it difficult to distinguish clear boundaries among these organs [4]. For this reason, and because we lack ultrastructural and functional data for photoreceptive organs of many cnidarian species, we refer to them all as eyes. Our ancestral state reconstruction strongly suggests

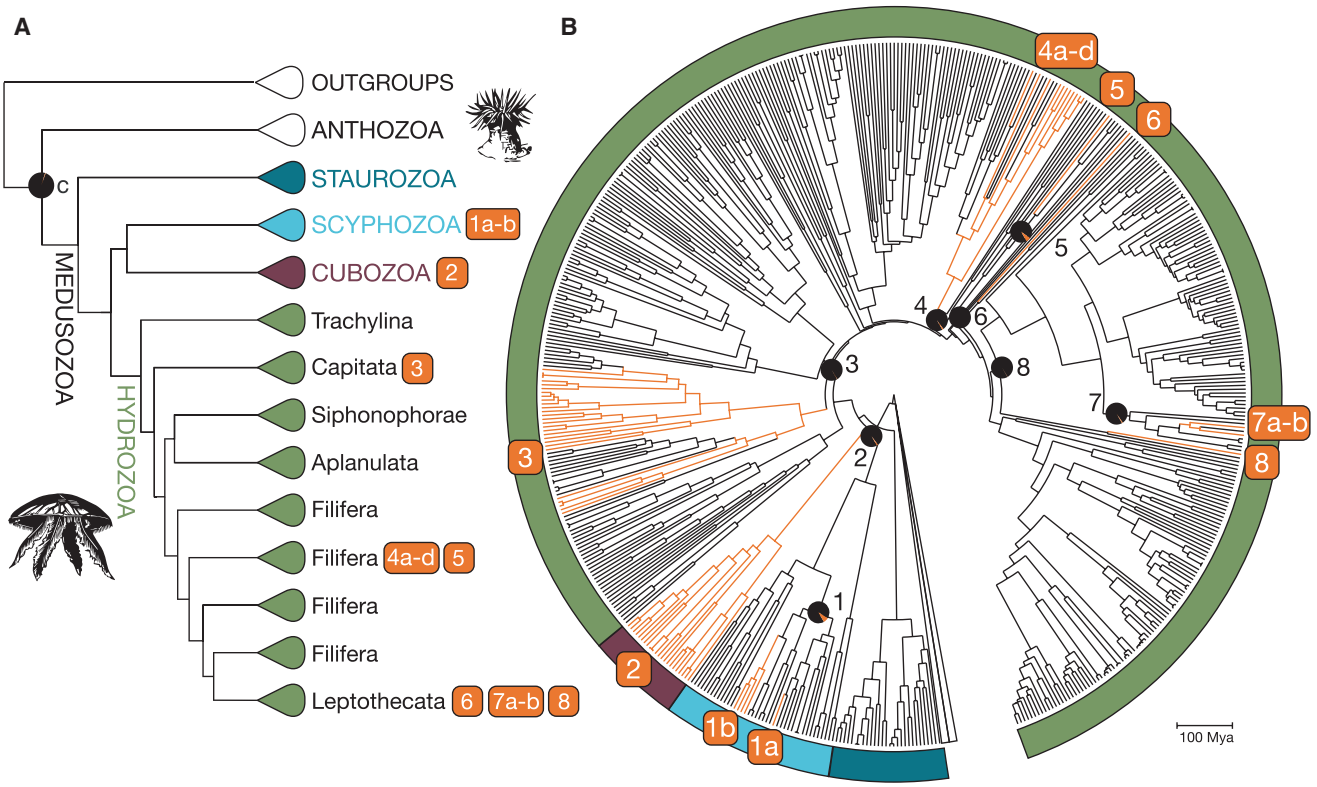

Figure 1. Eyes Originated between 8 and 13 Times in Cnidaria

(A) Summary of the cnidarian tree topology used for ancestral state reconstructions illustrated with major clades collapsed. The eyeless cnidarian ancestor is indicated as "c."

(B) Time-calibrated cnidarian tree with medusozoan clades expanded to show eye origins.

Eyes are only found in medusoid cnidarians, which have corresponding colors in (A) and (B). Pie charts at internal nodes represent selected ancestral states with marginal likelihoods for absence (black) and presence (orange) of eyes reconstructed using a two-state Markov model (1–7) ML estimate of transition rates was 0.08 (gains:losses). Numbers 1–8 in orange squares denote eight most conservative, separate origins of eyes mapped on the ML tree inferred from a concatenated dataset of five genes (18S, 28S, COI, 16S and 12S; 6,629 nucleotides) from 1,106 taxa (Anthozoa: 548, Medusozoa: 554, outgroups: 4) under a GTR+R10 model. We used TreePL to transform branch lengths to be proportional to time. Origins 1, 4, and 7 correspond to two or four eye origins as represented by "a," "b," "c," and "d" (see text for discussion). The Bayes factor test of independent origins strongly favors the alternative hypothesis (H_1) of at least eight origins as opposed to fewer than eight (H_0) (Bayes factor $H_0/H_1 = 9.3 \times 10^{-25}$). Orange branches represent transitions from eye absence to eye presence inferred with parsimony ancestral state reconstruction using the accelerated transformation criteria.

All node support values and ancestral state reconstructions are available in Figures S1 and S2. See also Table S1 and Data S1.

that the last common cnidarian ancestor (Figure 1A), as well as key ancestors in major medusozoan classes (Staurozoa, Scyphozoa, Cubozoa, and Hydrozoa), lacked eyes (Figure 1B). Thus, eyes probably originated repeatedly, at least eight times among distantly related medusoid cnidarians, and up to 16 times with less conservative counting of state transitions (Figure 1). First, reconstructions under parsimony indicate 10 to 16 origins of eyes as equally most parsimonious, depending on the transformation criterion (accelerated or delayed) (see supplemental results in Data and Software Availability in STAR Methods). Second, using ML, we estimated rates of character transitions assuming an asymmetric, two-state Markov model, generating marginal likelihoods for both states (presence or absence of eyes) at every internal node on our species phylogeny. Eyes originated 13 times in cnidarians under ML when counting character transitions where one state has a significantly higher proportion of marginal likelihood (Figures 1 and S1). More conservative counting leads to fewer inferences of eye gain. We conservatively infer one gain instead of more in each of two hydrozoan clades (gains 4 and 7 on Figure 1; see also Figure S1) where the likelihood of eye presence in some internal nodes was substantially, but not significantly, higher than absence. Furthermore, we conservatively infer one scyphozoan origin instead of two due to a lack of observations on eye for some species. In sum, even conservative counting of ML ancestral states infers eight origins, one in the lineage leading to box jellyfishes (Cubozoa), one in scyphomedusae (Scyphozoa), and six in hydromedusae (Hydrozoa). Finally, Bayesian character state analysis (Bayes factor test) supports the estimate of multiple eye origins in agreement with ML and parsimony results. The Bayes factor test of independent origins assumes known rates of gains and losses and a continuous-time Markov model of evolution. We compared the probability of observing our data under the hypothesis that eyes originated in Cnidaria less than eight times to the alternative hypothesis that eyes originated at least eight

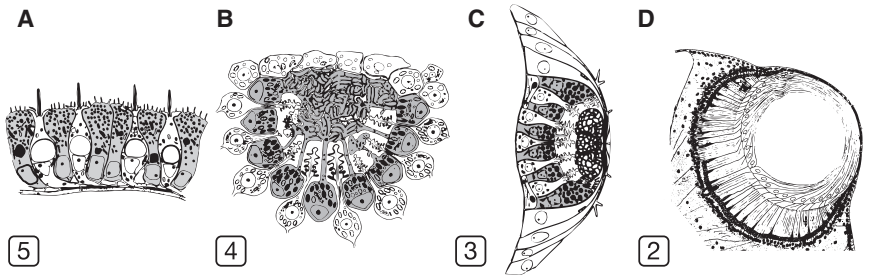

Figure 2. Eyes of Separate Origin Differ in Ultrastructural Details

(A) Eyespot from the hydrozoan *Leuckartiara octona* (Fleming 1823), Origin 5). Pigment and spindle-shaped photosensory ciliary cells alternate in a single layer, with ciliary cells having an exceptional supranuclear vacuole.

(B) Everted pigment cup from the hydrozoan *Bougainvillia principis* (Steenstrup 1850), Origin 4). Cuboidal pigment cells form a cup into which they project irregular tubular processes. Photosensory ciliary cells may bear one to three cilia, and their projections are spatially separated from those of the pigment cells.

(C) Everted pigment cup with lens from the hydrozoan *Cladonema radiatum* Dujardin 1843, Origin 3. Basal parts of the photosensory ciliary cells are located between the pigment cells and their distal parts project microvilli that intermingle with those of adjacent cells. Cytoplasmic portions of the pigment cells extend to form a compact lens.

(D) Lens eye of the cubozoan *Carybdea xaymacana* Conant 1897 (Origin 2). Cornea made of flattened ectodermal cells and spherical crystallin lens separated by a small space from a retina composed of columnar pigmented photosensory ciliary cells. Origin labels are in squares. Modified from [13, 15–17].

See also Table S1.

times. This led to a Bayes factor test consistent with ML and parsimony results, strongly favoring at least eight origins in Cnidaria across several priors on rates of eye gains and losses. Furthermore, the Bayes factor test still strongly and consistently favors hypotheses of more than a single origin, two origins, and four to five origins as suggested by previous studies on cnidarian eye evolution and also across several priors on gains and losses rates (see Table S2 of supplemental results in Data and Software Availability in STAR Methods).

We did not find our inferences of eye history to be sensitive to reasonable variations in the species tree. Most importantly, the Bayes factor test of independent origins incorporates uncertainty in species tree topology using a distribution of trees from bootstrapped pseudoreplicates of our molecular data using ML. Second, we considered multiple phylogenetic hypotheses from different analytical strategies, including data partitioning and varying outgroups (see STAR Methods for details). Most living cnidarians belong to two historically well-supported groups (but see [8]): Anthozoa (~7,500 species) and Medusozoa (~3,500 species). We excluded a third group recently confirmed to be cnidarians [9], the Myxozoa (~2,200 species), from our analyses because they are challenging to place phylogenetically without very large datasets, are extremely divergent from other lineages, and—as endoparasites—lack eyes. Despite consistent support for these three major groups in the literature, relationships within each are still contentious, and differences within Medusozoa in particular could impact our ancestral state estimations. Our analyses consistently place Staurozoa as sister to other medusozoan groups as suggested previously by rDNA analyses [10] but in disagreement with recent phylogenomic studies [11, 12]. However, differences in the phylogenetic relationships within medusozoan groups (especially within Hydrozoa) did not affect our conservative inference of at least eight origins of eyes in Cnidaria (see supplemental results in Data and Software Availability in STAR Methods).

Our model of evolution for ancestral state reconstruction relied on scoring cnidarian species as having eyes simply "present" or "absent." Differences in morphology and development of eyes in different cnidarian lineages offer additional data to address the hypothesis of eight eye origins and provide insight into the evolutionary processes that shaped eye evolution in cnidarians. Therefore, we compiled descriptions of fine structure and development of eyes. We find that morphological details are often different among eyes we infer to be of separate origin, as expected in the absence of strong convergent evolution. For example, Origin 1 includes scyphozoans *Aurelia aurita* Linnaeus 1758 (Origin 1a) and *Cassiopea xamachana* Bigelow 1892 (Origin 1b), whose eyes differ from those of other medusozoans in having pigmented photosensory cells [13, 14]. Origin 2 includes the unique and sophisticated lensed eye of box jellyfishes (Figure 2D), which have a three-layered retina, unique crystalline lens, and cornea [18, 19]. Although we count cubozoan eyes as having a single origin separate from other cnidarians, cubozoans themselves have multiple eye types, including pit and slit eyes and planular eyes in single individuals [20], all of which are absent in close relatives. Therefore, each of these eye types could have a separate origin if they are not derived from each other. Origins 3–8 encompass the eyes of hydrozoans, which comprise two cell types: pigment cells and photosensory ciliary cells. Origin 3 includes the everted pigment cup eyes of *Cladonema radiatum* Dujardin 1843 (Figure 2C), which have compact lenses formed of subunits from distal cytoplasmic portions of pigment cells that synthesize lens proteins [13, 15]. Origin 4 is represented by *Bougainvillia principis* (Steenstrup 1850), which also have everted pigment cup eyes (Figure 2B) that differ from those of Origin 3 in having a lens-like body (but without *Cladonema*-like subunits) formed from agglomerations of lateral projections of pigment cells, which are spatially separated from multiciliated photosensory cells [16]. Origin 5 includes *Leuckartiara octona* (Fleming 1823) (Figure 2A), in which the two cell types are interspersed in a single flat layer to form an eyespot [16]. Here, the photosensory cells are different from other cnidarian eyes in possessing an exceptional supranuclear vacuole and cilia without striated rootlets [16]. Origins 6 and 8 have never been the subject of ultrastructural work. Finally, Origin 7 is represented by inverted pigment cup eyes of *Tiaropsis multicirrata* (Sars 1835), which have ectodermal photosensory cells and endodermal pigment cells [16]. Several of the separate origins we postulate are consistent with Salvini-Plawen and Mayr [4],

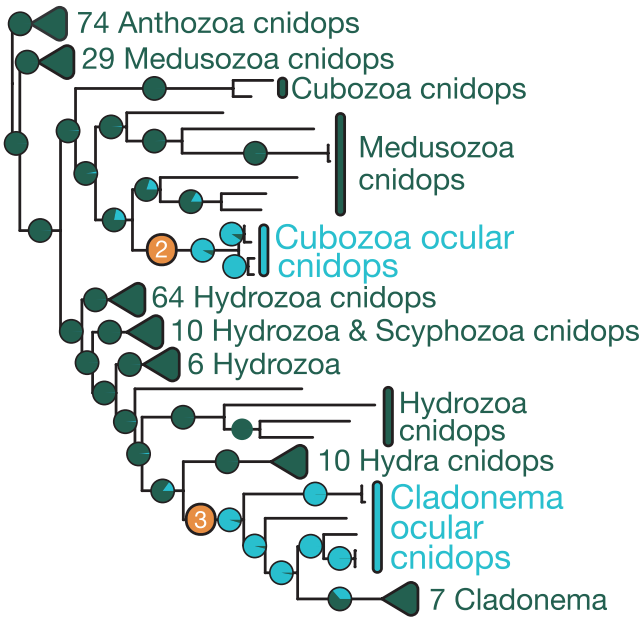

Figure 3. The Evolutionary History of Cnidarian Opsins Is Consistent with Multiple Eye Origins

We analyzed a large opsin dataset from all animals, including extensive new cnidarian sequences, with ML under a LG+F+R10 model in IQTREE. Illustrated here are cnidarian xenopsins [40] (cnidops [41]) and their pattern of ocular (light blue) and non-ocular (dark green) expression (see Figure S3 for full sequence names). Each pie chart displays the proportion of marginal likelihood for one state (ocular) versus the other (extraocular). Here, we also plot with orange squares separate origins of eyes from Cubozoa (box jellyfish; Origin 2) and *Cladonema* (Origin 3), species whose ocular opsins are known [27, 42–44]. The ocular opsins of Origin 2 and Origin 3 are distantly related to each other, and each is descended from extraocular opsins. The alternative hypothesis of homology of eyes from origins 2 and 3 would predict their ocular opsins to be closely related, forming a monophyletic group. An alternative cnidops topology as recovered with a ML analysis under a GTR+G model in RAxML is also consistent with these conclusions (see Figures S1, S2, and S3).

who lacked detailed phylogenetic hypotheses but posited our Origins 1, 2, 3, 5, and 7 based on morphology alone. Along with morphology, developmental genetic details differ between eyes that we infer to have separate origins. *Pax* genes are typically regulators of animal eye development, including cnidarians [3]. Whereas *Pax-B* is involved in the development of lensed eyes of the box jellyfish *Tripedalia cystophora* (Origin 2), *Pax-A* regulates the development of eyes in the hydrozoan *C. radiatum* (Origin 3) [3]. Our phylogenetic analyses shed new light on eye morphology, indicating that cnidarian eyes of separate origin evolved differently in morphological detail, perhaps using distinct developmental pathways.

Light Sensitivity Likely Predates Eye Origins in Cnidaria

In addition to strong support for separate origins of eyes, we find light sensitivity, the first step toward evolving an eye [21], to be present across all Cnidaria, not only those closely related to species with eyes. Light sensitivity is present in many eyeless organisms, which often perceive light through dispersed extraocular photoreceptor cells [22, 23] using various molecular mechanisms [24]. Extraocular light sensitivity is found in Cnidaria, which respond to light and use it to tune essential activities like larval settlement, spawning, migration, feeding, or cnidocyte firing. We compiled reports of light-associated processes for eyeless species in our tree (Data S1) to show that light sensitivity is widespread across all cnidarian classes. We made no attempt to distinguish different mechanisms, as these are usually unknown in cnidarians (but see [25, 26]). One genetic mechanism for light sensitivity is opsin-based phototransduction. Light sensitivity of opsin proteins has been tested directly in two cnidarian species [27, 28] and indirectly with electroretinograms in others [29–33]. Additionally, opsins were probably present in ancestral cnidarians [34–36]. Therefore, opsins serve as logical candidate genes for many extraocular light-sensing functions. Light-sensing functions across all cnidarian classes suggest that light sensitivity did not appear separately in groups with eyes but rather was likely ancestral, long predating all origins of all cnidarian eyes. Consequently, if light sensitivity existed in the first cnidarians, we speculate light sensitivity acted through dispersed, extraocular photoreceptor cells expressing opsins for any of a variety of functions. Ancestral photoreception is consistent with a traditional idea that eyes evolve stepwise, building upon ancestral photoreceptor cells over evolutionary time [37, 38].

Separate Co-option of Distantly Related Extraocular Opsins Supports Multiple Eye Origins

To test whether visual opsins are derived from extraocular genes in Cnidaria, as in bilaterian animals with central nervous systems [39], we inferred opsin history using new and published transcriptomes of 86 cnidarian species. Consistent with separate eye origins, we demonstrate that eyes from at least two different origins express distantly related opsin genes (Figure 3), and we show that opsins now expressed in eyes evolved from extraocular opsins (Figure 3).

To understand the history of ocular opsins, we tested two previous hypotheses of cnidarian opsin evolution using opsins from unprecedented taxonomic diversity, now including staurozoans, scyphozoans, siphonophores, and anthozoans. First, in an analysis including opsins from across all animals, we corroborate that all cnidarian opsins fall into three different subfamilies: chaopsins, anthozoa II opsins, and xenopsins [34, 40] (see supplemental results in Data and Software Availability in STAR Methods). We also corroborate that cnidarian xenopsins (also called cnidops [41]) are the only opsins known from medusozoans, the only cnidarians with eyes. We focused therefore on cnidops history to understand whether cnidarian eye origins were associated with separate co-option of extraocular genes. Following the cnidarian species tree, we find cnidops history to include an early divergence between anthozoan and medusozoan sequences, with opsins known to be expressed in cnidarian eyes belonging to the medusozoan opsin group (see full opsin tree in Figure S12 in supplemental results in Data and Software Availability in STAR Methods). With an alternative model of sequence evolution, GTR+G instead of LG+F+R10, cnidops topology is different, such that the medusozoan opsins no longer form a monophyletic group (see Figure S13 in supplemental results in Data and Software Availability in STAR Methods).

By analyzing the expression history of cnidops in or out of eyes, we infer that at least two separate eye origins, origins 2 and 3, were accompanied by shifts in opsin expression from extraocular to photoreceptor cells of newly evolved eyes (Figure 3). Using the cnidops topology obtained when using either GTR+G or LG+F+R10, our ancestral state estimates of cnidops expression shows that transitions from extraocular to ocular expression occurred separately when lensed eyes originated in *C. radiatum* (Origin 3) and in cubozoans *T. cystophora* Conant, 1897 and *Carybdea rastonii* Haake, 1886 (Origin 2). Therefore, opsin history agrees with our inferences of multiple origins of eyes, with separate origins reflected in repeated events of extraocular opsins becoming ocular. Alternatively, if eyes had originated only once among cnidarians, followed by multiple losses, we would expect to find ocular opsins from eyed species in a monophyletic group. That is, cnidops from the eyes of *Cladonema*, *Carybdea*, and *Tripedalia* would be closely related. Indeed, we find that *Carybdea* and *Tripedalia* ocular opsins form a monophyletic group, as expected, since their homologous eyes belong to Origin 2, and in turn are distantly related to *Cladonema* ocular opsins, present in eyes from Origin 3. Accordingly, our ML ancestor estimation infers separate transitions from extraocular expression to ocular in each of these groups.

Conclusions

Taken together, our results suggest cnidarian eyes evolved multiple times from ancestral photoreceptor cells, with opsins expressed in eyes of separate origin having evolved from divergent extraocular genes. These results make sense of previously published morphological and developmental details and make new predictions. Rather than representing stages of a single line of gradual evolution [16], cnidarian eyes originated prolifically in the absence of a central nervous system, often using different opsin paralogs, different morphological building blocks, and/or different developmental pathways. These perspectives provide rich opportunities to address fundamental evolutionary questions. To what extent are developmental, physiological, and genetic bases similar among cnidarian eyes within the same origin and different between origins? Do convergent eyes ever use the same developmental, physiological, or genetic basis? Do homologous cell types evolve differently in eyes versus outside of eyes, and if so, are cell types themselves convergent? The phylogenetic studies presented here provide a framework for such future studies.

STAR★METHODS

Detailed methods are provided in the online version of this paper and include the following:

SUPPLEMENTAL INFORMATION

Supplemental Information includes three figures, one table, and one data file and can be found with this article online at https://doi.org/10.1016/j.cub.2018.05.055.

ACKNOWLEDGMENTS

We thank Casey Dunn for suggestions on how to generate the cnidarian tree. We also thank Vladimir Minin and André Morandini for discussions and help with analytical tools. Professor Glen Watson kindly donated *Haliplanella* (=*Diadumene*) *luciae* specimens for transcriptome analysis. Alex Pulido helped with figures, and Nicholai Hensley contributed comments that improved the original manuscript. We thank David Plachetzki and Michael Broe for support with transcriptome files. Computer infrastructure was provided by the Center for Scientific Computing at UCSB and NSF grant CNS-0960316NSI, with assistance from Paul Weakliem and Burak Himmetoglu. This work was supported by CAPES (Coordenação de Aperfeiçoamento de Pessoal de Nível Superior) through a doctoral scholarship to N.P. (Process BEX-13130-13/7) in the program Science without Borders. T.H.O and M.D. acknowledge funding from the National Science Foundation through grants DEB-1354831, IOS-1456859, and DEB-1257796.

AUTHOR CONTRIBUTIONS

Conceptualization, N.P. and T.H.O.; Methodology, N.P., M.D.R., and T.H.O.; Investigation, N.P., J.R.K., N.S., N.G.R., and J.T.C.; Software, A.J.M.S.; Resources, A.J.M.S, M.D.R., and M.D.; Data Curation, N.P.; Visualization, N.P. and T.H.O.; Writing—Original Draft, N.P. and T.H.O.; Writing—Review & Editing, N.P., T.H.O., N.S., M.D., M.D.R., and J.R.K.; Supervision, N.P. and T.H.O.; Funding Acquisition, N.P., T.H.O., and M.D.

DECLARATION OF INTERESTS

The authors declare no competing interests.

Received: January 10, 2018
Revised: March 26, 2018
Accepted: May 17, 2018
Published: July 19, 2018

REFERENCES

1. Oakley, T.H., and Speiser, D.I. (2015). How Complexity Originates: The Evolution of Animal Eyes. Annu. Rev. Ecol. Evol. Syst. *46*, 237–260.
2. Garm, A., Ekström, P., Boudes, M., and Nilsson, D.-E. (2006). Rhopalia are integrated parts of the central nervous system in box jellyfish. Cell Tissue Res. *325*, 333–343.
3. Suga, H., Tschopp, P., Graziussi, D.F., Stierwald, M., Schmid, V., and Gehring, W.J. (2010). Flexibly deployed Pax genes in eye development at the early evolution of animals demonstrated by studies on a hydrozoan jellyfish. Proc. Natl. Acad. Sci. USA *107*, 14263–14268.
4. Salvini-Plawen, L., and Mayr, E. (1977). On the evolution of photoreceptors and eyes. In Evolutionary Biology, M. K. Hecht, W. C. Steere, and B. Wallace, M.A. Boston, ed. (US: Springer), pp. 207–263.
5. Marques, A.C., and Collins, A.G. (2004). Cladistic analysis of Medusozoa and cnidarian evolution. Invertebr. Biol. *123*, 23–42.
6. Arendt, D., and Wittbrodt, J. (2001). Reconstructing the eyes of Urbilateria. Philos. Trans. R. Soc. Lond. B Biol. Sci. *356*, 1545–1563.

7. Nilsson, D.-E. (2004). Eye evolution: a question of genetic promiscuity. Curr. Opin. Neurobiol. *14*, 407–414.
8. Kayal, E., Roure, B., Philippe, H., Collins, A.G., and Lavrov, D.V. (2013). Cnidarian phylogenetic relationships as revealed by mitogenomics. BMC Evol. Biol. *13*, 5. https://doi.org/10.1186/1471-2148-13-5.
9. Chang, E.S., Neuhof, M., Rubinstein, N.D., Diamant, A., Philippe, H., Huchon, D., and Cartwright, P. (2015). Genomic insights into the evolutionary origin of Myxozoa within Cnidaria. Proc. Natl. Acad. Sci. USA *112*, 14912–14917.
10. Collins, A.G., Schuchert, P., Marques, A.C., Jankowski, T., Medina, M., and Schierwater, B. (2006). Medusozoan phylogeny and character evolution clarified by new large and small subunit rDNA data and an assessment of the utility of phylogenetic mixture models. Syst. Biol. *55*, 97–115.
11. Zapata, F., Goetz, F.E., Smith, S.A., Howison, M., Siebert, S., Church, S.H., Sanders, S.M., Ames, C.L., McFadden, C.S., France, S.C., et al. (2015). Phylogenomic analyses support traditional relationships within Cnidaria. PLoS ONE *10*, e0139068.
12. Kayal, E., Bastian, B., Pankey, M.S., Ohdera, A., Medina, M., Plachetzki, D.C., Collins, A., and Ryan, J.F. (2017). Comprehensive phylogenomic analyses resolve cnidarian relationships and the origins of key organismal traits. PeerJ Preprints. https://doi.org/10.7287/peerj.preprints.3172v1.
13. Bouillon, J., and Nielsen, M. (1974). Etude de quelques organes sensoriels de cnidaires. Arch. Biol. (Liege) *85*, 307–328.
14. Yamasu, T., and Yoshida, M. (1973). Electron microscopy on the photoreceptors of an anthomedusa and a scyphomedusa. Publ. Seto Mar. Biol. Lab. *20*, 757–778.
15. Weber, C. (1981). Structure, histochemistry, ontogenetic development, and regeneration of the ocellus of Cladonema radiatum Dujardin (Cnidaria, Hydrozoa, Anthomedusae). J. Morphol. *167*, 313–331.
16. Singla, C.L. (1974). Ocelli of hydromedusae. Cell Tissue Res. *149*, 413–429.
17. Berger, E.W., Berger, E.H., and Conant, F.S. (1900). Physiology and histology of the Cubomedusae, including Dr. F.S. Conant's notes on the physiology ... / (The John Hopkins Press).
18. Yamasu, T., and Yoshida, M. (1976). Fine structure of complex ocelli of a cubomedusan, Tamoya bursaria Haeckel. Cell Tissue Res. *170*, 325–339.
19. O'Connor, M., Garm, A., Marshall, J.N., Hart, N.S., Ekström, P., Skogh, C., and Nilsson, D.-E. (2010). Visual pigment in the lens eyes of the box jellyfish Chiropsella bronzie. Proc. Biol. Sci. *277*, 1843–1848.
20. Nordström, K., Wallén, R., Seymour, J., and Nilsson, D. (2003). A simple visual system without neurons in jellyfish larvae. Proc. Biol. Sci. *270*, 2349–2354.
21. Nilsson, D.-E. (2013). Eye evolution and its functional basis. Vis. Neurosci. *30*, 5–20.
22. Ramirez, M.D., Speiser, D.I., Pankey, M.S., and Oakley, T.H. (2011). Understanding the dermal light sense in the context of integrative photoreceptor cell biology. Vis. Neurosci. *28*, 265–279.
23. Sumner-Rooney, L., Rahman, I.A., Sigwart, J.D., and Ullrich-Lüter, E. (2018). Whole-body photoreceptor networks are independent of 'lenses' in brittle stars. Proc. Biol. Sci. *285*, 20172590. https://doi.org/10.1098/rspb.2017.2590.
24. Porter, M.L. (2016). Beyond the Eye: Molecular Evolution of Extraocular Photoreception. Integr. Comp. Biol. *56*, 842–852.
25. Plachetzki, D.C., Fong, C.R., and Oakley, T.H. (2012). Cnidocyte discharge is regulated by light and opsin-mediated phototransduction. BMC Biol. *10*, 17.
26. Levy, O., Appelbaum, L., Leggat, W., Gothlif, Y., Hayward, D.C., Miller, D.J., and Hoegh-Guldberg, O. (2007). Light-responsive cryptochromes from a simple multicellular animal, the coral Acropora millepora. Science *318*, 467–470.
27. Koyanagi, M., Takano, K., Tsukamoto, H., Ohtsu, K., Tokunaga, F., and Terakita, A. (2008). Jellyfish vision starts with cAMP signaling mediated by opsin-G(s) cascade. Proc. Natl. Acad. Sci. USA *105*, 15576–15580.
28. Quiroga Artigas, G., Lapébie, P., Leclère, L., Takeda, N., Deguchi, R., Jékely, G., Momose, T., and Houliston, E. (2018). A gonad-expressed opsin mediates light-induced spawning in the jellyfish *Clytia*. eLife *7*, e29555.
29. Weber, C. (1982). Electrical activities of a type of electroretinogram recorded from the ocellus of a jellyfish, Polyorchis penicillatus (Hydromedusae). J. Exp. Zool. *223*, 231–243.
30. Weber, C. (1982). Electrical activity in response to light of the ocellus of the ocellus of the hydromedusan, Sarsia tubulosa. Biol. Bull. *162*, 413–422.
31. Coates, M.M., Garm, A., Theobald, J.C., Thompson, S.H., and Nilsson, D.-E. (2006). The spectral sensitivity of the lens eyes of a box jellyfish, Tripedalia cystophora (Conant). J. Exp. Biol. *209*, 3758–3765.
32. Ekström, P., Garm, A., Pålsson, J., Vihtelic, T.S., and Nilsson, D.E. (2008). Immunohistochemical evidence for multiple photosystems in box jellyfish. Cell Tissue Res. *333*, 115–124.
33. Garm, A., Coates, M.M., Gad, R., Seymour, J., and Nilsson, D.-E. (2007). The lens eyes of the box jellyfish Tripedalia cystophora and Chiropsalmus sp. are slow and color-blind. J. Comp. Physiol. A Neuroethol. Sens. Neural Behav. Physiol. *193*, 547–557.
34. Feuda, R., Hamilton, S.C., McInerney, J.O., and Pisani, D. (2012). Metazoan opsin evolution reveals a simple route to animal vision. Proc. Natl. Acad. Sci. USA *109*, 18868–18872.
35. Plachetzki, D.C., Fong, C.R., and Oakley, T.H. (2010). The evolution of phototransduction from an ancestral cyclic nucleotide gated pathway. Proc. Biol. Sci. *277*, 1963–1969.
36. Feuda, R., Rota-Stabelli, O., Oakley, T.H., and Pisani, D. (2014). The comb jelly opsins and the origins of animal phototransduction. Genome Biol. Evol. *6*, 1964–1971.
37. Oakley, T.H., and Sabrina Pankey, M. (2008). Opening the "Black Box": The Genetic and Biochemical Basis of Eye Evolution. Evolution. Evol. Educ. Outreach *1*, 390–402.
38. Nilsson, D.E., and Pelger, S. (1994). A pessimistic estimate of the time required for an eye to evolve. Proc. Biol. Sci. *256*, 53–58.
39. Porter, M.L., Blasic, J.R., Bok, M.J., Cameron, E.G., Pringle, T., Cronin, T.W., and Robinson, P.R. (2012). Shedding new light on opsin evolution. Proc. Biol. Sci. *279*, 3–14.
40. Ramirez, M.D., Pairett, A.N., Pankey, M.S., Serb, J.M., Speiser, D.I., Swafford, A.J., and Oakley, T.H. (2016). The last common ancestor of most bilaterian animals possessed at least nine opsins. Genome Biol. Evol. *8*, 3640–3652.
41. Plachetzki, D.C., Degnan, B.M., and Oakley, T.H. (2007). The origins of novel protein interactions during animal opsin evolution. PLoS ONE *2*, e1054.
42. Suga, H., Schmid, V., and Gehring, W.J. (2008). Evolution and functional diversity of jellyfish opsins. Curr. Biol. *18*, 51–55.
43. Liegertová, M., Pergner, J., Kozmiková, I., Fabian, P., Pombinho, A.R., Strnad, H., Pačes, J., Vlček, Č., Bartůněk, P., and Kozmik, Z. (2015). Cubozoan genome illuminates functional diversification of opsins and photoreceptor evolution. Sci. Rep. *5*, 11885.
44. Bielecki, J., Zaharoff, A.K., Leung, N.Y., Garm, A., and Oakley, T.H. (2014). Ocular and extraocular expression of opsins in the rhopalium of Tripedalia cystophora (Cnidaria: Cubozoa). PLoS ONE *9*, e98870.
45. Van Dongen, S.M. (2000). Graph clustering by flow simulation. Available at: https://dspace.library.uu.nl/handle/1874/848.
46. Yang, Y., and Smith, S.A. (2014). Orthology inference in nonmodel organisms using transcriptomes and low-coverage genomes: improving accuracy and matrix occupancy for phylogenomics. Mol. Biol. Evol. *31*, 3081–3092.
47. Katoh, K., and Standley, D.M. (2013). MAFFT multiple sequence alignment software version 7: improvements in performance and usability. Mol. Biol. Evol. *30*, 772–780.
48. Capella-Gutiérrez, S., Silla-Martínez, J.M., and Gabaldón, T. (2009). trimAl: a tool for automated alignment trimming in large-scale phylogenetic analyses. Bioinformatics *25*, 1972–1973.

49. Oakley, T.H., Alexandrou, M.A., Ngo, R., Pankey, M.S., Churchill, C.K.C., Chen, W., and Lopker, K.B. (2014). Osiris: accessible and reproducible phylogenetic and phylogenomic analyses within the Galaxy workflow management system. BMC Bioinformatics *15*, 230.
50. Nguyen, L.-T., Schmidt, H.A., von Haeseler, A., and Minh, B.Q. (2015). IQ-TREE: a fast and effective stochastic algorithm for estimating maximum-likelihood phylogenies. Mol. Biol. Evol. *32*, 268–274.
51. Lanfear, R., Frandsen, P.B., Wright, A.M., Senfeld, T., and Calcott, B. (2017). PartitionFinder 2: new methods for selecting partitioned models of evolution for molecular and morphological phylogenetic analyses. Mol. Biol. Evol. *34*, 772–773.
52. Smith, S.A., and O'Meara, B.C. (2012). treePL: divergence time estimation using penalized likelihood for large phylogenies. Bioinformatics *28*, 2689–2690.
53. Beaulieu, J.M., O'Meara, B.C., and Donoghue, M.J. (2013). Identifying hidden rate changes in the evolution of a binary morphological character: the evolution of plant habit in campanulid angiosperms. Syst. Biol. *62*, 725–737.
54. Pankey, M.S., Minin, V.N., Imholte, G.C., Suchard, M.A., and Oakley, T.H. (2014). Predictable transcriptome evolution in the convergent and complex bioluminescent organs of squid. Proc. Natl. Acad. Sci. USA *111*, E4736–E4742.
55. Maddison, W.P., and Maddison, D.R. (2018). Mesquite: a modular system for evolutionary analysis.
56. Bolger, A.M., Lohse, M., and Usadel, B. (2014). Trimmomatic: a flexible trimmer for Illumina sequence data. Bioinformatics *30*, 2114–2120.
57. Grabherr, M.G., Haas, B.J., Yassour, M., Levin, J.Z., Thompson, D.A., Amit, I., Adiconis, X., Fan, L., Raychowdhury, R., Zeng, Q., et al. (2011). Full-length transcriptome assembly from RNA-Seq data without a reference genome. Nat. Biotechnol. *29*, 644–652.
58. Haas, B.J., Papanicolaou, A., Yassour, M., Grabherr, M., Blood, P.D., Bowden, J., Couger, M.B., Eccles, D., Li, B., Lieber, M., et al. (2013). De novo transcript sequence reconstruction from RNA-seq using the Trinity platform for reference generation and analysis. Nat. Protoc. *8*, 1494–1512.
59. Speiser, D.I., Pankey, M.S., Zaharoff, A.K., Battelle, B.A., Bracken-Grissom, H.D., Breinholt, J.W., Bybee, S.M., Cronin, T.W., Garm, A., Lindgren, A.R., et al. (2014). Using phylogenetically-informed annotation (PIA) to search for light-interacting genes in transcriptomes from non-model organisms. BMC Bioinformatics *15*, 350.
60. Stamatakis, A. (2014). RAxML version 8: a tool for phylogenetic analysis and post-analysis of large phylogenies. Bioinformatics *30*, 1312–1313.
61. Fu, L., Niu, B., Zhu, Z., Wu, S., and Li, W. (2012). CD-HIT: accelerated for clustering the next-generation sequencing data. Bioinformatics *28*, 3150–3152.
62. Larsson, A. (2014). AliView: a fast and lightweight alignment viewer and editor for large datasets. Bioinformatics *30*, 3276–3278.
63. Kainer, D., and Lanfear, R. (2015). The effects of partitioning on phylogenetic inference. Mol. Biol. Evol. *32*, 1611–1627.
64. Bergsten, J. (2005). A review of long-branch attraction. Cladistics *21*, 163–193.
65. Park, E., Hwang, D.S., Lee, J.S., Song, J.I., Seo, T.K., and Won, Y.J. (2012). Estimation of divergence times in cnidarian evolution based on mitochondrial protein-coding genes and the fossil record. Mol. Phylogenet. Evol. *62*, 329–345.
66. Van Iten, H., Marques, A.C., Leme, J. de M., Pacheco, M.L.A.F., and Simões, M.G. (2014). Origin and early diversification of the phylum Cnidaria Verrill: major developments in the analysis of the taxon's Proterozoic–Cambrian history. Palaeontology *57*, 677–690.
67. Cunningham, J.A., Liu, A.G., Bengtson, S., and Donoghue, P.C.J. (2017). The origin of animals: Can molecular clocks and the fossil record be reconciled? BioEssays *39*, 1–12.
68. Morandini, A.C., and Marques, A.C. (2010). Revision of the genus Chrysaora Péron and Lesueur, 1810 (Cnidaria: Scyphozoa). Zootaxa *2464*, 1–97.
69. Fewkes, J.W. (1882). Notes on Acalephs from the Tortugas, with a description of new genera and species. Bull. Mus. Comp. Zool. *9*, 251–290.
70. Russell, F.S. (1970). The Medusae of British Isles (Cambridge University Press).
71. Martin, M. (2011). Cutadapt removes adapter sequences from high-throughput sequencing reads. EMBnet.journal *17*, 10–12.
72. Ahrendt, S.R., Medina, E.M., Chang, C.A., and Stajich, J.E. (2017). Exploring the binding properties and structural stability of an opsin in the chytrid *Spizellomyces punctatus* using comparative and molecular modeling. PeerJ *5*, e3206.
73. Li, W.-H., Yang, J., and Gu, X. (2005). Expression divergence between duplicate genes. Trends Genet. *21*, 602–607.
74. Mooers, A.Ø., and Schluter, D. (1999). Reconstructing ancestor states with maximum likelihood: support for one-and two-rate models. Syst. Biol. *48*, 623–633.
75. Pagel, M. (1999). The maximum likelihood approach to reconstructing ancestral character states of discrete characters on phylogenies. Syst. Biol. *48*, 612–622.

STAR★METHODS

KEY RESOURCES TABLE

REAGENT or RESOURCE	SOURCE	IDENTIFIER
Deposited Data		
Haliplanella luciae (=Diadumene lineata) transcriptome	This paper	SRA: SRP152591, BioProject: PRJNA464357
Renilla koellikeri transcriptome	This paper	SRA: SRP152591, BioProject: PRJNA464357
Opsin sequences	This paper	GenBank: MH586782-MH586815
Software and Algorithms		
MCL 14-137	[45]	https://micans.org/mcl/
Blast-to-MCL (python script)	[46]	https://bitbucket.org/yangya/phylogenomic_dataset_construction
Write-fasta-files-from-MCL (python script)	[46]	https://bitbucket.org/yangya/phylogenomic_dataset_construction
Seqmatcher (python script)		https://bitbucket.org/swafford
MAFFT 7.304b	[47]	https://mafft.cbrc.jp/alignment/software/
trimAl 1.2	[48]	http://trimal.cgenomics.org
Remove phytab dupes	[49]	galaxy-dev.cnsi.ucsb.edu/osiris
Phylocatenator	[49]	galaxy-dev.cnsi.ucsb.edu/osiris
IQTREE 1.4.2	[50]	http://www.iqtree.org
PartitionFinder2	[51]	http://www.robertlanfear.com/partitionfinder/
TreePL 1.0	[52]	https://github.com/blackrim/treePL
corHMM (R package)	[53]	https://github.com/thej022214/corHMM
Indorigin (R package)	[54]	https://github.com/vnminin/indorigin
Mesquite 1.0	[55]	http://www.mesquiteproject.org
Trim Galore 0.4.2		http://www.bioinformatics.babraham.ac.uk/projects/trim_galore/
Trimmomatic 0.32	[56]	http://www.usadellab.org/cms/?page=trimmomatic
Trinity 2.2.0	[57]	https://github.com/trinityrnaseq/trinityrnaseq/wiki
TransDecoder r2012-08-15	[58]	https://github.com/TransDecoder/TransDecoder/wiki
PIA (Phylogenetically Informed Annotation)	[59]	http://galaxy-dev.cnsi.ucsb.edu/pia/
RAxML versions 8.2.9 and 7.4.3	[60]	https://sco.h-its.org/exelixis/web/software/raxml/
Supercuts (python script)		https://bitbucket.org/swafford/supercuts
CD-HIT 4.6	[61]	http://weizhongli-lab.org/cd-hit/
AliView 1.18	[62]	http://www.ormbunkar.se/aliview/
trimAl 1.2	[48]	http://trimal.cgenomics.org
Other		
Resource website for the publication (sequence data, analyses, and resources related to the species and opsin tree reconstructions)	This paper	https://github.com/npicciani/picciani_et_al_2018

CONTACT FOR REAGENT AND RESOURCE SHARING

Further information and request for resources and reagents should be directed to and will be fulfilled by the Lead Contact, Todd H. Oakley (oakley@lifesci.ucsb.edu).

EXPERIMENTAL MODEL AND SUBJECT DETAILS

Animals

Polyps of *Haliplanella luciae* (Verrill, 1898) (= *Diadumente lineata*) used for transcriptome analysis were maintained in natural seawater at room temperature (22°C ± 1°C) under a 12:12 h photoperiod. Using a seawater open system (16°C ± 2°C; 12:12 h photoperiod), we

cultivated colonies of *Renilla koellikeri* Pfeffer, 1886 (Anthozoa, Pennatulacea), collected in the Santa Barbara Channel on June 10th 2015. We fed the animals with 3-day-old Selcon enriched *Artemia* nauplii (San Francisco Strain Brine Shrimp Eggs).

METHOD DETAILS

Dataset assembly for species tree

We first retrieved DNA sequences (43,667) for all taxonomically non-redundant cnidarians available in the nucleotide database of NCBI on 10-26-2016. The database contains many taxonomically redundant sequences from the following: *Nematostella vectensis*, *Hydra oligactis, Hydra vulgaris, Corallium, Faviina, Porites, Stylophora, Acropora, Anthopleura elegantissima, Aiptasia, Aurelia aurita, Exaiptasia pallida* and *Hydractinia symbiolongicarpus.* In order to reduce computation time, we analyzed sequences from these taxa (120,554; also retrieved on 10-26-2016) separately in a second round of clustering analyses as explained below.

Because previous studies often sequenced non-overlapping portions of homologous genes, we inferred clusters of homologous gene regions from these bulk downloads as described in [46]. We initially built a local blast database and performed all-against-all searches to recover pairwise similarity scores among sequences. After excluding BLAST results without a 50% minimum sequence overlap to avoid short sequences (with the python script 'blast-to-mcl'; [46]), we clustered remaining sequences using MCL 14-137 (Markov Clustering Algorithm [45];) with an inflation value of 2.0. We converted the MCL output to fasta files using the python script 'write-fasta-files-from-mcl' after shortening sequence names in the original fasta file [46]. Sequence names were matched back using a python script "seqmatcher" (available at http://bitbucket.org/swafford/). By manually inspecting the resulting clusters, we selected those that encompassed a taxonomically diverse range of cnidarians. More specifically, we did not consider clusters with sequences from only one species, one genus or two genera for further analyses, unless clusters were not monospecific and contained species for which light sensing information is available. Most representative genes were partial regions of the 12S, 16S, cytochrome oxidase subunit 1 (COI) mtDNA in addition to 18S and 28S rDNA genes. After determining the suite of genes to be groomed in this first set of analyses, we repeated the clustering protocol with the molecular dataset from the highly redundant taxa originally excluded. Sequence clusters with any of those genes were then merged with the selected raw clusters from the primary dataset for a third round of clustering analyses. In this third clustering analysis, we used a combination of 0.4 minimum sequence coverage for exclusion and 1.4 MCL inflation value for large but still alignable clusters.

We aligned genes with only one cluster each (18S and 12S) using MAFFT 7.305b (L-INS-i). Other genes (28S, 16S, COI) had taxa spread out in multiple clusters most likely due to sequencing of distinct regions of the same molecular marker. We merged clusters corresponding to the same gene and aligned the merged file using MAFFT 7.305b (E-INS-i), which accounts for multiple alignable and long unalignable regions among sequences [47]. We trimmed low quality regions of each gene alignment using trimAl 1.2 [48] by removing positions with gaps in 40% or more sequences. Next, we removed spurious sequences by retaining only those with at least 65% nucleotides achieving a 60% overlap with those from other sequences. Merging 28S clusters resulted in a poor quality alignment with no sequences retained after using trimAl. Therefore, instead of merging 28S clusters, we selected the most taxonomically diverse 28S cluster to align, trim, and use for downstream analyses. We then discarded redundant sequences (keeping the longest sequence for a species, gaps ignored when counting nucleotide bases) with the tool "remove_phytab_dupes" ([49]; available at Osiris on the Galaxy Bioinformatics Platform; http://galaxy-dev.cnsi.ucsb.edu/osiris). We concatenated processed alignments using Phylocatenator (also available at Osiris), retaining species with at least two genes. We manually included sequences from the following outgroup species: *Crassostrea gigas*, *Amphimedon queenslandica*, *Strongylocentrotus purpuratus* and *Trichoplax adhaerens*. With the concatenated dataset (GenBank accession numbers in Table S3 of supplemental results in Data and Software Availability), we performed a preliminary maximum likelihood analysis and excluded unstable long-branch taxa (myxozoan species, *Juncella fragilis*, *Lepidisis olapa*, *Leptogorgia virgulata* and *Acropora* sp.).

SPECIES TREE RECONSTRUCTION

With this final dataset (1106 terminal taxa, 6629 aligned nucleotides), we performed model selection and maximum likelihood analyses using IQ-TREE multicore 1.4.2 [50] and explored the effects of partitioning to accommodate variation in substitution rates among sites and inclusion of distantly related outgroups on tree topology, branch lengths and node supports (see [63, 64]). We therefore analyzed our dataset with 4 strategies: (1) without partitioning, (2) with partitioning, (3) without partitioning and no outgroup, (4) with partitioning and no outgroup. When we partitioned the dataset, we selected the best partitioning scheme and evolutionary models using PartitionFinder2 [51]. We measured branch support in trees from all strategies with the ultrafast bootstrap algorithm, aBayes and SH-aLRT on 1,000 replicates using IQ-TREE. According to BIC (Bayesian Information Criterion), the best model for the unpartitioned dataset under strategies (1) and (3) was GTR+R10, and GTR+I+G for a partition of mitochondrial genes and SYM+I+G for that of nuclear genes under (2) and (4). Maximum likelihood analyses were run for a total of 10 replicates under each strategy. Trees without the outgroups were rooted with Anthozoa, as the split between Anthozoa and Medusozoa is well supported and we were mostly interested in the topology changes among medusozoan groups (see main text for discussion). We time-calibrated the main tree shown in Figure 1 before ancestral state reconstruction using penalized likelihood with six fossil calibrations in TreePL 1.0 [52]. Within Cnidaria, we used fossil calibration dates from Park et al. [65], with the exception of family Rhizangiidae, for which we had no sequence data. We chose min and max dates for crown group Cnidaria from Van Iten et al. [66], and for the root of the tree, we used 635 Ma as the lower bound for Metazoa based on biomarker evidence as per Cunningham [67]. Species names, genes and

accession numbers of sequences concatenated for species tree are available at a github repository, as well as supplemental results from strategies 2-4 (see Data and Software Availabilitysection below).

We scored cnidarians in our phylogeny as possessing eyes or not based on an extensive literature survey (Table S1), with eyes defined minimally as a region with alternating pigment and photoreceptor cells (also called ocelli). One caveat of our scoring is that many species accounts are based on preserved material, which may lose pigmentation due to fixatives and hinder the recognition of eyes (A. Morandini, personal communication). Nonetheless, high quality descriptions with fresh material show that many scyphozoans (e.g., *Chrysaora* spp.) truly lack eyes in their rhopalia [68] and taxonomic descriptions typically state explicitly when eyes are absent in the species. Considering the lack of mention of ocelli could be due to fixative issues, we assigned a missing state to species of scyphozoans and hydrozoans that had no mention of ocelli in descriptions, recognizing a possibility for absence or presence of eyes in those (see observations in Table S1). Pigment spots are often associated with light sensitivity, but their role in light perception needs to be validated with experimental or ultrastructural evidence. The broad scale of our analysis required us to rely on several observations made with light microscopy, so that in many cases we lack direct evidence for light perception. At present, there is therefore a fair amount of uncertainty on whether all cnidarian eyes are functional. Nonetheless, our phylogenetic results show that many eyes for which we do not have direct experimental evidence of light perception belong to close relatives of species that possess well-studied eyes (e.g., those shown in Figure 3).

Besides the adult medusae, other life stages can also be very active, such as the free-swimming planula larvae and the young scyphozoan medusae or ephyra. Detailed studies describe single-cell pigment cups in the planula of cubozoans despite their lack of a nervous system [20]. Among scyphozoans, if the adult is eyeless, their ephyra tends to be eyeless as well (see [69]. For instance, the ephyra of the scyphozoan *Pelagia noctiluca* (Forsskål, 1775) bears no eyes and remains eyeless as an adult medusa (Hertwig 1878, after [70]), but the opposite occurs in *Aurelia aurita* (Linnaeus, 1758) and *Nausithoe aurea* Silveira & Morandini 1997, whose eyes start developing in the young ephyra and reach full size in the adult medusa [14]. Although eyes in other stages will substantially add to our knowledge on cnidarian eye evolution, we restrict this study to eyes in the well-studied adult medusae in order to facilitate a broad scale analysis.

RNA-Seq library preparation and sequencing

For 9 anemone species (*Actinia equina*, *Aiptasia pallida*, *Anthopleura elegantissima*, *Bunodosoma cavernata*, *Calliactis parasitica*, *Metridium senile*, *Sargatia elegans*, *Stomphia coccinea, Triactis producta*), tissue excised from the polyp was flash frozen in liquid nitrogen and stored at −80°C. Total RNA was extracted using the RNeasy Mini Kit (QIAGEN), following manufacturer-supplied protocols. Small (1.5-2.0 mm), sterile ceramic beads were added to each sample along with Buffer RLT and then each tissue sample was homogenized using a Mini-Beadbeater-8 (BioSpec Products). RNA extractions were quantified on the Qubit 2.0 (Life Technologies) and RIN values determined on the BioAnalyzer (Agilent Technologies). First strand synthesis, library construction, and paired-end 100 base sequencing were conducted at The Genomics Shared Resource Center of the The Ohio State University James Comprehensive Cancer Center (Columbus, OH, USA). For *Haliplanella luciae* (= *Diadumene lineata*) and *Renilla koellikeri*, total RNA from polyp tentacles was extracted using the Nucleospin RNA II kit (Macherey-Nagel) or the QIAGEN RNEasy Mini kit. First and second strand cDNA synthesis was made with the SMARTer cDNA Kit and Advantage 2 PCR kits (Clontech). Libraries were constructed using the Illumina TruSeq kit and sequencing was performed on Illumina HiSeq 2000 and 3000 platforms.

Dataset assembly for opsin tree

To identify candidate opsin genes, we screened 109 transcriptomes of 86 cnidarian species, including 98 deposited in the NCBI SRA (Sequence Read Archive; NCBI) and TSA (Transcriptome Shotgun Assembly; NCBI) databases and 11 newly generated datasets (species and accession numbers listed in Table S4 of supplemental results in Data and Software Availability). Paired or single-end raw reads from the SRA and newly generated reads were trimmed for quality (minimum Phred score of 33) and adaptors (automatically detected) using either Trim Galore 0.4.2 [a wrapper for Cutadapt 1.12 [71] and FastQC 0.11.5] or Trimmomatic 0.32 [56] followed by assembly using Trinity 2.2.0 [57, 58]. We detected open reading frames with at least 30 amino acids among transcripts in each transcriptome using TransDecoder r2012-08-15 [58]. We used PIA [59] to identify candidate opsin genes. We modified PIA to include a reduced opsin bait set with two or three sequences (one deuterostome, one protostome and one cnidarian representative if applicable) of each opsin group described in Ramirez et al. [40]. For initially estimating the placement of candidate sequences we used the opsin dataset of [34], which comprises cnidarian opsin sequences and non-opsin GPCR outgroups. We performed blastp searches against the transcriptomes using the opsin bait set with an e-value of 1e-10 and added all candidate opsin sequences onto Feuda's master opsin alignment with MAFFT-profile. With the evolutionary placement algorithm implemented in RAxML 8.2.9 [60], we placed new candidate opsin sequences on Feuda's tree using a maximum likelihood criterion. We used the python script "supercuts" (available at https://bitbucket.org/swafford/supercuts) to retain cnidarian query sequences closely related to opsins, placopsins and melatonin receptors for further phylogenetic analysis. We used tblastn to blast all the selected candidate opsin protein sequences against the 2014 NCBI nucleotide database on Galaxy Platform and removed potential contaminants (observed to match queries with unexpected highly significant e-values and identity; available at at the github repository in the file "contaminants.fasta"). We also removed redundant duplicates and partial sequences for each species in our cnidarian dataset using CD-HIT 4.6 [61] with an identity threshold of 100% (final set of candidate opsin sequences in Table S5 of supplemental results in Data and Software Availability).

Opsin tree reconstruction

We added all sequences from [40] and representatives of melatonin receptors, placopsins and chytropsins [72] as outgroups to our cnidarian dataset as these are some of the closest groups to canonical type-II opsins [34]. We rooted our opsin trees with the chytropsins. We removed duplicates from the cnidarian species that were already in the Ramirez dataset using AliView 1.18 [62] and aligned the final opsin dataset using MAFFT 7.304b (E-INS-i [47];). We used trimAl 1.2 [48] to remove positions with gaps in 90% or more sequences and spurious sequences that did not have 65% of their residues achieving an overlap of 50% with those of other sequences. Our final alignment consisted in 1591 protein sequences and 457 amino acid residues. We carried out model selection and tree reconstruction under a maximum likelihood (ML) criteria using IQ-Tree multicore 1.4.2 [50]. We performed 35 ML searches under the LG+F+R10 model. We measured branch support using the Ultrafast Bootstrap (UFBoot) algorithm with 1000 replicates, the SH-aLRT and abayes (approximate transformation Bayes test). The ultrafast bootstrap support values did not converge in the best ML search, therefore we re-ran an extra search with the best tree as a starting tree and ensured the UFBoot values converged (i.e., achieving a bootstrap correlation coefficient of split occurrence frequencies > 0.99). In addition to the LG+F+R10 model, we reconstructed the opsin tree using the GTR+G model in RaxML 7.4.3 [60] and generated bootstrap values based on 100 replicates.

After generating the opsin phylogeny, we restricted the ancestral state reconstruction to the cnidops subfamily. As such, we used the cnidops topology to reconstruct the location of expression for ancestral cnidops sequences, whether it was ocular or non-ocular. Our scoring considered not only the sample from which the transcriptome was generated but also *in situ* hybridization data on opsin expression from previous studies. We considered ocular opsins to be those expressed in photoreceptor cells of eyes, and non-ocular those expressed outside photoreceptor cells of eyes (Table S6 of supplemental results in Data and Software Availability). When an opsin sequence is expressed ubiquitously across body regions including photoreceptor cells (which only is known from *Cladonema*), we scored it as polymorphic or ambiguous as it is both non-ocular and ocular. Note also that many cnidarians are eyeless, and in instances where we find opsins in those species, we called them non-ocular without the need for data on localization. While common to conduct ancestral state reconstruction on time-calibrated trees, as we did for Cnidarian species, we did not scale branch lengths to time for the opsin gene tree because constraining nodes with fossils requires confident identification of orthologs, which is challenging for opsins [40] Instead of attempting a rough chronogram to map the history of opsin expression, we scaled branch lengths by amino acid substitutions in opsins. This assumes shifts in location of gene expression location are reflected by substitution rates, reasonable because expression divergence is often correlated with sequence divergence [73]. We estimated the ancestral states (ocular versus non ocular expression) across the opsin phylogeny as described below (see Quantification and Statistical Analysis). We used an asymmetric Markov two-state model (transition rates different) given its best fit compared to a symmetric Markov two-state model according to a likelihood ratio analysis (chi-square test; df = 1; $p < 0.05$).

QUANTIFICATION AND STATISTICAL ANALYSIS

To statistically infer ancestral states, we used the function RayDISC in the R package ''corHMM'' to compute the marginal state likelihoods at internal nodes in rooted species trees [53]. When the state is missing or the species is polymorphic, RayDISC assigns equal likelihoods to both states (presence or absence of eyes). We compared the fit of two models of character evolution, an asymmetric Markov two-state model (transition rates different) and a symmetric Markov two-state model (equal transition rates), to our data. A Markov transition rate model of evolution assumes the probability of change of a character does not depend on previous states, that character transition along a branch is independent of transitions in other parts of the tree, and that rates of transition do not change along the branches of a tree [74]. Our likelihood ratio test indicates a significantly better fit of an asymmetric Markov two-state model to our data under the topologies of all species tree reconstruction strategies (chi-square test; df = 1; $p < 0.05$ for all topologies). For each ancestral node, we considered the marginal likelihood of eye presence (P) to be significantly better than the marginal likelihood of eye absence (A) when $|\ln(P) - \ln(A)| > 2$ [75]. Because we were only able to include very distantly related outgroups, we did not score them for eyes and used a root prior that assumes equal likelihoods for both states (presence and absence of eyes). Additionally to these likelihood reconstructions, we accounted for phylogenetic uncertainty in cnidarian relationships and used the R package ''indorigin'' to perform a Bayes Factor Test of Independent Origins comparing the probability of the observed data under the null and alternative hypothesis of less or at least a specified number of origins, with a set of 1,000 bootstrap replicates produced under strategy 1 (unpartitioned analysis, described above) with estimated transition rates from corHMM (see more details about the Bayes Factor Test in [54]). Parsimony ancestral state reconstruction was made with Mesquite 1.0 [55]. Finally, we gathered reports of light-associated processes among cnidarians in our phylogenetic dataset from the literature (Data S1).

DATA AND SOFTWARE AVAILABILITY

The accession numbers for opsin sequences and transcriptomes generated in this study are GenBank: MH586782-MH586815, SRA: SRP152591 in BioProject PRJNA464357. Additional method details, sequences and analytical results (including supplemental results referenced throughout the main text) are available at https://github.com/npicciani/picciani_et_al_2018.